

An analysis of Southeastern US prescribed burn weather windows: seasonal variability and El Niño associations

A. M. Chiodi^{A,C}, N. S. Larkin^B and J. Morgan Varner^B

^AJoint Institute for the Study of the Atmosphere and Ocean, University of Washington and NOAA Pacific Marine Environmental Laboratory, Seattle, WA 98115, USA.

^BPacific Wildland Fire Sciences Laboratory, USDA Forest Service, Seattle, WA 98103, USA.

^CCorresponding author. Email: andy.chiodi@noaa.gov

Abstract. Fire plays an important role in wildland ecosystems, critical to sustaining biodiversity, wildlife habitat and ecosystem health. By area, 70% of US prescribed burns take place in the Southeast, where treatment objectives range widely and accomplishing them depends on finding specific weather conditions for the effective and controlled application of fire. The climatological variation of the preferred weather window is examined here using two weather model reanalyses, with focus on conditions critical to smoke dispersion and erratic fire behaviour. Large spatial gradients were evident in some months (e.g. 3× change across the Appalachian Mountains in winter). Over most of the Southeast, availability of preferred conditions in summer was several (up to 8) times less than in autumn or winter. We offer explanation for this variability in terms of the mean seasonal changes of key weather conditions (especially mixing height and transport wind). We also examine the interannual variability of the preferred weather window for linkage to the tropical Pacific (1979–2010). Associations with the subset of El Niño events identified by outgoing-longwave-radiation suggest skilful seasonal fire weather forecasts are feasible. Together, these findings offer a predictive tool to prioritise allocation of scarce prescribed fire resources and maximise annual area treated across this landscape.

Additional keywords: climatology, mixing height, prescribed burns, Southeast, transport winds.

Received 24 August 2017, accepted 11 January 2018, published online 28 March 2018

Introduction

Prescribed burns are an essential tool for forest managers to maintain ecosystem health and function, and to reduce the risk of large wildfires (Ryan *et al.* 2013). Nearly 70% of the total US prescribed burn activity, by area, takes place within the South-eastern USA (hereafter ‘Southeast’) (Melvin 2015), where fire is applied to wildland forests and grasslands to foster a wide range of management objectives, many of which are associated with a preferred season for treatment. Typical objectives include the maintenance and restoration of threatened and endangered species, the restoration and maintenance of wildlife habitat, the reduction of potentially hazardous levels of wildland fuels, and controlling woody competition in stands managed for timber (see Wade and Lunsford 1989 or Waldrop and Goodrick 2012 for a more complete list).

To accomplish these objectives, prescribed burns are used under the specific wind, fuel and moisture conditions conducive to the effective yet controlled application of fire. Limited availability of the preferred fire weather conditions, especially in regard to their effect on smoke management, and thus breathable air quality, have been cited as a primary barrier to reaching the desired levels and timings of prescribed burn activity (Haines *et al.* 2001; Kobziar *et al.* 2015).

The goals of the present study are to improve current understanding of the extent to which the prescribed burn weather window varies with location and season over the Southeast. We also examine the drivers of this variability in terms of the interplay between changes in the respective atmospheric conditions and their preferred ranges. We use data from two numerical weather models run in data-assimilation mode (‘reanalyses’) to examine the historical variability of the preferred weather window over the 1979–2010 period, with focus on the near-surface dispersion conditions critical to effective smoke management. From this perspective, limits on the available weather window correspond at the low end of the preferred range to atmospheric circulation levels minimally sufficient to disperse enough smoke to maintain breathable air quality and supply the prescribed burns with oxygen. The upper limit of the preferred range corresponds to conditions in which erratic fire behaviour is known to occur and prescribed burns risk becoming difficult to control.

Atmospheric mixing height and transport wind, along with indices calculated based on them (e.g. atmospheric dispersion index, Lavdas 1986; ventilation index, Hardy *et al.* 2001, Goodrick *et al.* 2013), are currently the fundamental variables used to estimate near-surface dispersion conditions for smoke

management purposes in the Southeast (Goodrick *et al.* 2013). Mixing height has been defined as the height above ground to which ground-released pollutants will disperse based on ambient circulation (including turbulent and convective components; Seibert *et al.* 2000; Fearon *et al.* 2015). Transport wind is calculated as the vertical average of wind speed from the surface to the mixing height. We base our main calculation here on the preferred range of mixing height and transport wind over the study region. We use the thresholds suggested by Wade and Lunsford (1989), which continue to be applicable throughout the region: specifically, mixing height between 1700 and 6500 feet (~518–1918 m) above ground and transport wind between 9 and 20 mph (~4–9 m s⁻¹). Informed by the study of Fearon *et al.* (2015), which evaluated several mixing height estimation methods based on weather model data relative to a satellite-based lidar validation technique, we use the surface air parcel equilibrium approach, inclusive of the effects of humidity on parcel buoyancy, to estimate mixing height. The equilibrium height approach was found to be quantitatively very similar to other viable options (Richardson number and turbulent kinetic energy based schemes) when humidity effects are included, and is commonly used in operational settings in the study region (e.g. Brown and Hall 2010).

Additionally, we screened our base case prescribed burn day window for other weather conditions that might prevent a prescribed burn from taking place. These conditions include very low near-surface relative humidity ($\leq 20\%$) and very high near-surface wind speeds [20 ft (6.1 m) wind speed > 20 mph (9 m s⁻¹)], both of which increase the difficulty of controlling the applied fire. We also examine the frequency at which the times that are good for prescribed burning from a smoke dispersion perspective become unavailable because of daily rain amounts sufficient to make burns inefficient. We use the > 6.35 mm day⁻¹ (~0.25 inch day⁻¹) threshold here, as in Chiodi *et al.* (2016).

We also examine the interannual variability of the preferred weather conditions and its possible linkage to El Niño events in the tropical Pacific. Our approach was informed by the outgoing-longwave-radiation (OLR) El Niño perspective previously described in a series of papers by Chiodi and Harrison (2010, 2013, 2015). Initial motivation for using OLR, rather than other more traditional variables (such as sea surface temperature, or sea level pressure) to monitor the state of air–sea coupling in the tropical Pacific is that, of these measures, OLR is more closely related to the tropical atmospheric heating anomalies that allow the anomaly state of the tropical Pacific to influence extra-tropical seasonal weather conditions, including temperature and precipitation anomalies over the USA. The subset of El Niño years identified by the associated OLR El Niño index have been shown to account for nearly all of the useful (highly statistically significant, and consistent from event-to-event) US seasonal temperature (Chiodi and Harrison 2013; Harrison and Chiodi 2017) and precipitation (Chiodi and Harrison 2013, 2015) associations, over the time for which OLR information has been available from satellites. Strong links have been found previously between the OLR-identified El Niño years and wintertime precipitation anomaly over the Southeast. The present study examines whether similar linkages extend to the fire weather variables that we are interested in here.

Materials and methods

The core atmospheric variables needed to calculate mixing height and transport wind were obtained from two reanalysis products. One is the North American Regional Reanalysis (NARR) described by Mesinger *et al.* (2006) and available at $\sim 1/3^\circ$ latitude \times $1/3^\circ$ longitude resolution on a Northern Lambert Conformal Conic grid. The surface area contained in a NARR grid box over the study region (~ 1150 square km at 32°N) approximates the average area of the National Weather Service fire weather zones that span the Southeast, and for which forecasts are issued and permitting is often based. Thus, the NARR horizontal resolution is usefully adequate for our purposes. NARR offers analysis product variables at 3-h intervals, including 1500, 1800 and 2100 hours Coordinated Universal Time (UTC) (1000, 1300 and 1600 hours Eastern Standard Time, EST), and 29 pressure levels, with spacing of 25 hPa from 1000 to 700 hPa, and 50 hPa thereafter. NARR data were obtained from the National Oceanographic and Atmospheric Administration (NOAA) Earth System Research Laboratory (ESRL) Boulder, CO, USA (available at <http://www.esrl.noaa.gov/psd>, accessed 1 April 2017).

We also use the National Centers for Environmental Prediction Climate Forecast System Reanalysis (CFSR) 6-hourly product, described by Saha *et al.* (2010) and available at <https://rda.ucar.edu/datasets/ds093.0>, accessed 1 April 2017). In this case, the variables required to calculate mixing height and transport winds are available at 0.5° longitude \times 0.5° latitude horizontal resolution and analysed products are available four times per day (0000, 0600, 1200 and 1800 hours UTC) and from the period spanning 1979 to 2010. The vertical resolution of CFSR is similar to NARR with 25-hPa spacing between 1000 and 750 hPa, and 50-hPa spacing above 750 hPa.

Owing to their ability to resolve the effects of surface cooling at night, the evening-through-early-morning reanalysis time steps have very few times that exhibit mixing heights in the desired range; a stable vertical potential temperature (a proxy for air density) profile at night and early morning is instead the norm (e.g. Fig. 1a). Because of this (along with the associated fact that prescribed burns primarily take place during the day) we base our analysis on the available mid-morning-to-afternoon analysis product time steps, namely 1500, 1800 and 2100 hours UTC for NARR, and 1800 hours UTC for CFSR. A base study period of 1979–2010 is used in each case, with interannual anomalies calculated based on month or season by subtracting the respective monthly or seasonal average calculated over the full study period.

We used the equilibrium height approach to estimate mixing height. Equilibrium height is calculated as the height above ground to which an air parcel heated to the surface temperature would rise (in the case that it is buoyant compared with surrounding air) before it becomes neutrally buoyant at some higher altitude. The equilibrium height method is commonly used by National Weather Service Forecast Offices when issuing mixing height forecasts, and has been found to provide an effective estimate for the mixing height, especially when virtual potential temperature (as used by Stull 1991), rather than potential temperature (as used by Holzworth 1964, 1967) is used as proxy for air density when determining the surface air

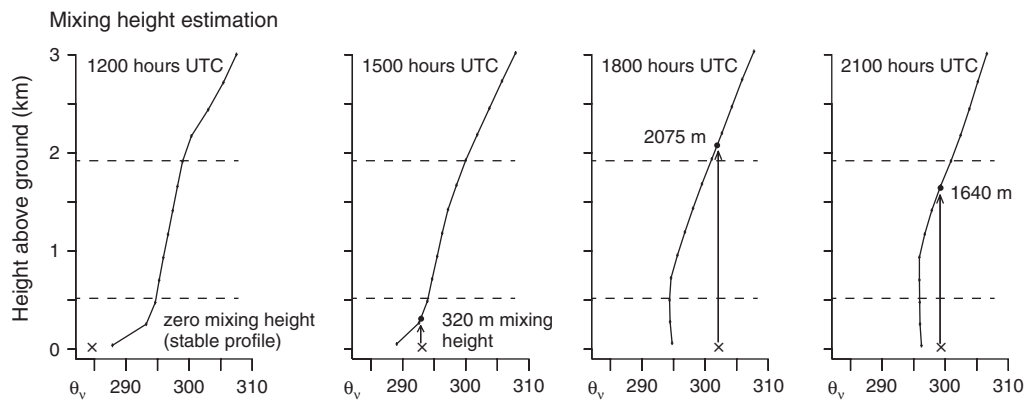


Fig. 1. Illustration of mixing height estimation method based on North American Regional Reanalysis (NARR) data for 1 January 2000, at 32°N, 90°W. Each panel shows the virtual potential temperature profile (θ_v , K), surface θ_v (x at surface height), estimated mixing height (black dot, when defined), and the preferred mixing height range (dashed lines). Arrows represent hypothetical ascent of a ground level air parcel heated to the surface temperature. In this case, only the conditions at 2100 hours Coordinated Universal Time (UTC) happen to meet the preferred criteria.

parcel's buoyancy (Fearon *et al.* 2015). The difference here being that humidity effects (which increase virtual potential temperature relative to potential temperature when water vapour is present) on air density would be ignored to an often misleading extent if using just potential temperature, rather than virtual potential temperature.

The variables acquired from the NARR for calculating mixing height are the pressure level analyses of temperature, specific humidity and geopotential height, as well as surface potential temperature, 2-m specific humidity and surface elevation. Standard formulae (e.g. Stull 1988, pp. 7, 276 and 551) were then used to compute vertical profiles of virtual potential temperature at each horizontal analysis product grid point, along with the ground surface virtual potential temperature. The calculation procedure for CFSR is similar to NARR, except that the surface temperature provided by CFSR is absolute rather than potential, meaning that the downloaded surface temperature variable from CFSR is first converted to potential temperature, before virtual surface potential temperature is calculated (even though the effect of not doing this is small in this case because we use a near-surface (1000 hPa) reference pressure). Fig. 1 illustrates example virtual potential temperature profiles and the associated mixing height estimation based on NARR data for 1 January 2000 at a selected Southeastern USA grid point (32°N, 90°W).

Profiles of zonal and meridional wind were also acquired from the NARR and CFSR reanalyses and used to calculate transport wind at each time step and grid point. Transport wind is defined as the vertically averaged wind speed from the ground to the mixing height, such that the product of the two base variables (often referred to as the ventilation index; Hardy *et al.* 2001; Goodrick *et al.* 2013) offers an estimate of the volume into which ground-released pollutants disperse upon mixing.

We also acquired 2 m relative humidity and 10-m wind speed from the NARR and CFSR reanalyses. The 10 m wind speed was divided by 1.15 to estimate the 20-foot wind speed (as in Turner and Lawson 1978), which is the commonly referred to measure of unobstructed near surface wind speed in the study region in the fire weather context.

The Daily USA Unified Precipitation dataset from the NOAA CPC (Higgins *et al.* 2000) is used to identify 24-h accumulations (starting 1200 hours UTC) greater than 0.25 inch (~6.35 mm). The dataset was obtained from the NOAA ESRL, Boulder, CO (available at <http://www.esrl.noaa.gov/psd>) and employs a Cressman-type objective analysis to provide daily values of precipitation based on station data on a horizontal grid with a spacing of 0.25° latitude and 0.25° longitude. The precipitation data were re-gridded to the NARR and CFSR horizontal grids before analysis, and all reanalysis time steps within the daily accumulation period were flagged as unavailable for prescribed burning when the 0.25 inch day⁻¹ threshold was met or exceeded.

The statistical significance of the El Niño composite anomalies was estimated using a bootstrap–Monte Carlo approach that relies on random sampling, with replacement, of the 32-year (1979–2010) record. Similar methods were used by Chiodi and Harrison (2013, 2015). The naming convention of years with regard to the seasonally locked life cycle of El Niño events that is used here is consistent with the seminal El Niño–Southern Oscillation Studies (Rasmusson and Carpenter 1983; Ropelewski and Halpert 1996), in which ‘Year 0’ corresponds to the seasons typically associated with onset and growth of El Niño events (Larkin and Harrison 2002) and ‘Year 1’ the following (e.g. for the 1982–83 El Niño, 1982 is Year 0 and 1983 Year 1). El Niño events typically peak, in terms of their tropical Pacific anomaly state, at approximately the end of Year 0 or beginning of Year 1.

We examined multiple sub-regions of the Southeast simultaneously to evaluate different types of seasonal weather variability. In such cases, it is important to also examine the associated composite anomalies for their overall regional statistical significance. This requires testing the null hypothesis that the amount of locally statistically significant anomaly contained in the regional composite can be explained by the effects of chance alone (e.g. when the 90% confidence interval is used in local statistical significance tests, and many different locations are tested, 10% of these locations should be expected to reach

Prescribed-burn-window climatology based on preferred mixing height (MH) and transport wind conditions

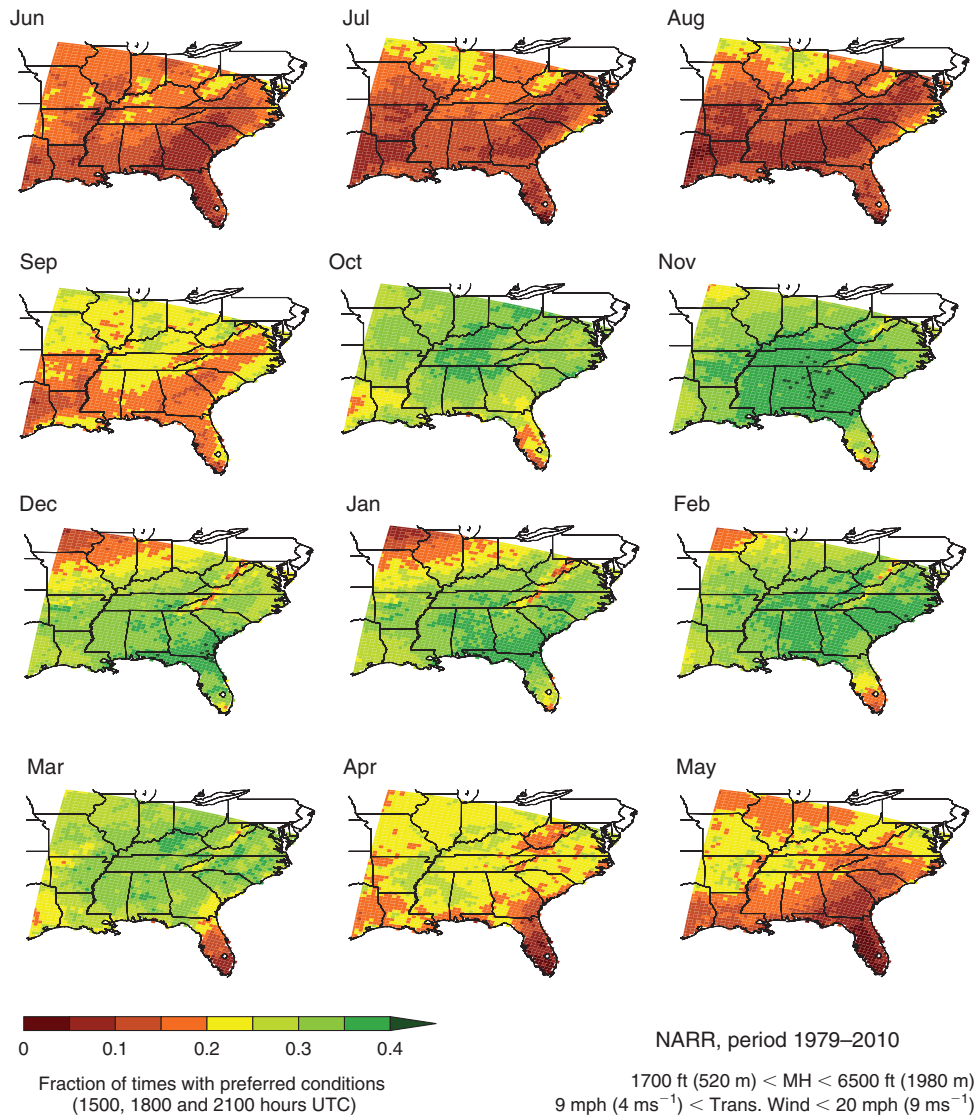


Fig. 2. Climatological monthly average prescribed burn window, based on frequency of co-occurring, preferred atmospheric boundary layer mixing height (MH) and transport wind conditions. Calculated based on North American Regional Reanalysis (NARR) data (period 1979–2010).

statistical significance based on chance alone, on average). We also use a Monte Carlo approach to test for statistical significance in the regional sense (as done and explained in more detail in [Chiodi and Harrison 2013, 2015](#)).

Results

Seasonal cycle

The mean seasonal progression of the prescribed burn weather window, based on preferable mixing height and transport wind conditions calculated from NARR data, varies widely across the Southeast ([Fig. 2](#)). Over most of the Southeast, the fraction of times available for prescribed burn treatment exhibits a low

point in summer; there was an all-region-average minimum of 13% in August. Substantially larger fractions of times are available for treatment in the dormant seasons. The all-region average reached a maximum of 34% in November. Transitions between the relatively narrow summertime window and more open winter conditions occurred, in a regionally averaged sense, in early autumn and spring ([Fig. 2](#)).

Different sub-regions within the Southeast, however, exhibited a seasonal cycle with somewhat different character than the full-region average. For example, lands just east of the Cumberland Plateau (e.g. central Kentucky and Tennessee) are fastest, in a climatological average sense, to transition out of the summertime minimum, reaching >35% availability in

October. This is while other sub-regions, especially some of those at lower latitude, are still much nearer their (low) summertime average. The north-western-most portion of the domain shown (e.g. Missouri, northern Illinois and Indiana) also experiences a distinct seasonal cycle, with peaks in October and March, separated by a low point in winter, which is when most of the study domain experiences a seasonally large number of prescribed burn preferable times.

The amplitude of the seasonal range varies with location and has a broad maximum centred over Georgia, extending to the surrounding states of Alabama, South Carolina and (northern) Florida, along with another over east Texas and Louisiana. In these locations, the monthly maximum and minimum values vary by a factor of five to seven from one another (c.f. August and November). A smaller seasonal range of values is experienced in the north-western part of the domain, including portions of Illinois and Indiana, where the monthly maximum and minimum differ from one another by only about a factor of two (c.f. October peak and March, or June minima).

A great deal of spatial variability is also evident within many of the individual months. In January, for example, the available percentage of times varies from 5 to 42%, depending on location, with higher availabilities observed over most of the south-eastern portion of the study area (the exception being land in or near the Florida Everglades), whereas much lower values are concentrated along the eastern flanks of the central Appalachian Mountains (i.e. the strip of red–yellow shading through West Virginia, Virginia, and North Carolina in Fig. 2). Lower values are also found more broadly across the north-western portion of the study region.

The companion CFSR set of results (Fig. 3) confirms the general seasonality of the prescribed burn weather window exhibited in Fig. 2, including the generally lower availability of preferred conditions in summer, and better availability in winter in most locations, with the exception of north-western portion of the domain (as is also the case based on NARR). There are, however, some differences apparent between the NARR- and CFSR-based results upon closer inspection. For example, the depression of preferred conditions along the eastern flanks of the Appalachian Mountains is more clearly seen in the NARR than CFSR case, perhaps because of the higher spatial resolution of the NARR data. There is also an overall increase in availability based on CFSR data, compared with the NARR result. This increase is perhaps most clearly seen by comparing the respective transition seasons (c.f. September, or April, based on NARR *v.* CFSR). Aspects of behaviour over the Florida Peninsula and east Texas also clearly depend on the dataset chosen in several months (e.g. October, March).

Why the preferred window varies seasonally

There are four primary ways in which the mixing height and transport wind conditions can fall outside of the preferred window: (i) mixing height (and by definition transport wind) is undefined because of stable atmospheric conditions; (ii) mixing height is outside the preferred range (either higher or lower), even though transport wind conditions are within range; (iii) transport wind alone is outside the preferred range; or (iv) transport wind and mixing height fall outside the preferred range simultaneously. Fig. 4 shows the result of tabulating the

frequency of each of these four possibilities for July, October, January and April (the centre months of the traditional 3-month seasons). The tabulation is done in this case over just the non-preferable time steps, such that the values shown along each row (month) sum to unity.

The upper row shows that when non-preferred conditions occur in July, the distribution of possible reasons depends on location, with non-preferred mixing heights being the most common (~50%; yellow shading in Fig. 4) in two sub-regions; one centred over North Carolina, including portions of the Atlantic Coastal Plain and Piedmont Plateau, and another centred over Missouri. Along much of the Gulf Coast, however, mixing height and transport wind evidently tend to more often fall out of range simultaneously. These results also show, perhaps unsurprisingly, that in mid-summer it is rare that the mixing height is undefined during the day due to a stable vertical density profile.

In October, there is an increase, compared with summer, in times during which the transport winds alone prevent the overall preferred conditions from being reached. This is especially the case over the north central portion of the study region and the eastern flanks of the Appalachian Mountains.

Out-of-range transport winds remain the most common reason for non-preferable conditions in January over most of the Southeast, with maxima over south-east Georgia, north-east Florida and the Appalachian Mountains. Over the more north-western reaches, however, stable atmospheric profiles become a contributing factor (~25% of cases) in January.

In April, stable profiles are no longer found in appreciable numbers, and it is a mix of transport winds and mixing heights that cause conditions to fall outside the preferred window, with wind (height) more often the case in the more north-western (south-eastern) part of the study region.

The comparable CFSR results (Fig. 5) agree with those based on NARR in that transport winds alone are generally the most common cause of non-preferable conditions in winter, whereas mixing height and transport wind conditions more evenly account for the non-preferable times in the spring and summer. Closer inspection, however, again reveals some quantitative differences between the NARR and CFSR results. In October, for example, stable profiles account for a somewhat greater fraction of the non-preferable times in the CFSR than NARR case, and above threshold (as will be shown below) mixing heights are more common based on NARR than CFSR, especially over east Texas and the Florida Peninsula. These differences are directly attributable to mixing heights calculated based on NARR being higher than those calculated based on CFSR. Inspection has revealed that there are clear discrepancies between the NARR and CFSR surface temperature fields at these times and locations (e.g. warmer surface temperatures based on NARR than based on CFSR, especially, over east Texas and Florida in October), which provide a proximate explanation for there being higher mixing heights in the NARR than CFSR case. This suggests that current uncertainty in our knowledge of surface temperature conditions contribute meaningful levels of uncertainty to our knowledge of the historical record of mixing height. Notwithstanding these particulars, it is reassuring that the CFSR results have largely the same character as the NARR results.

Prescribed-burn window climatology based on preferred mixing height (MH) and transport wind conditions

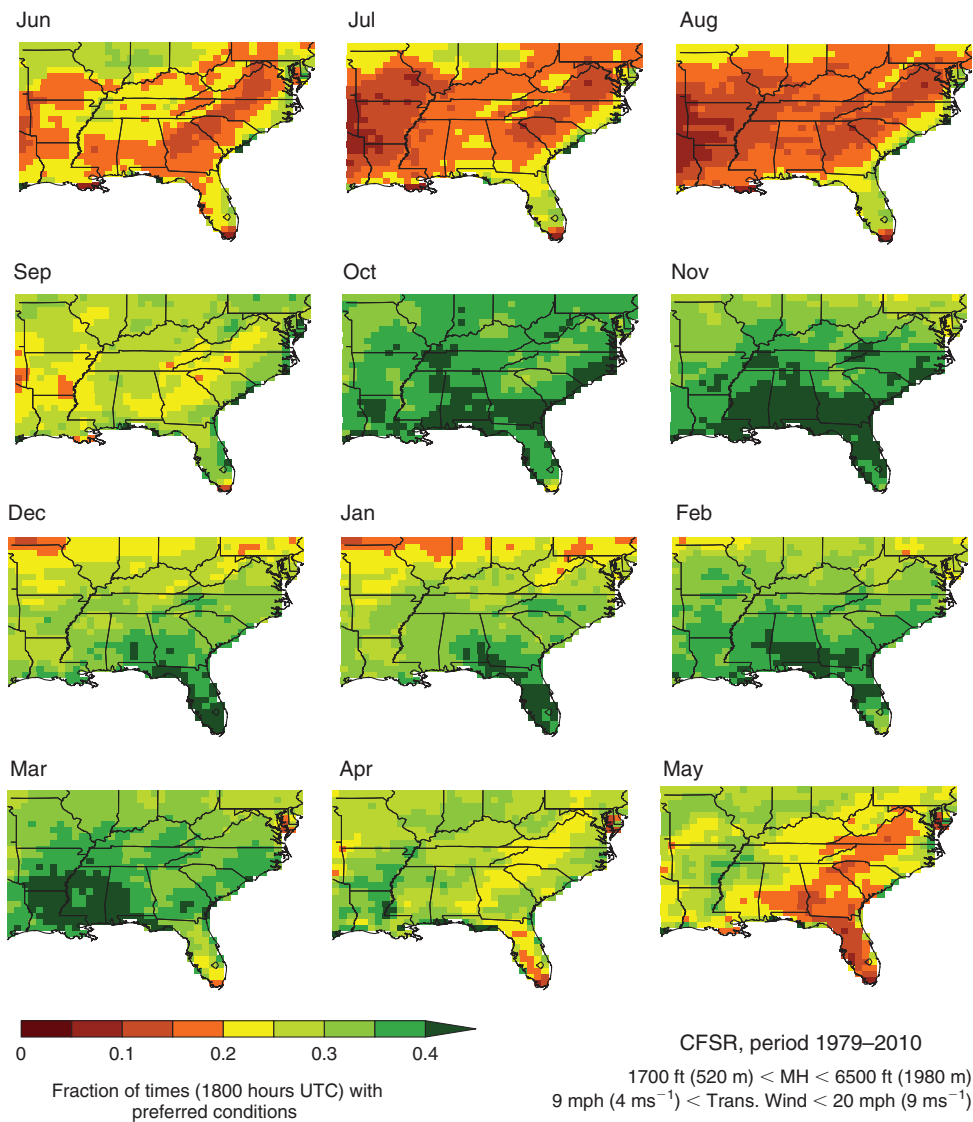


Fig. 3. Climatological monthly average prescribed burn window, based on frequency of co-occurring, preferred atmospheric boundary layer mixing height (MH) and transport wind conditions. Calculated based on Climate Forecast System Reanalysis (CFSR) data (period 1979–2010).

The manner in which mixing height and transport winds tend to fall outside the preferred range (i.e. are either too large or too small) is illustrated based on NARR data in Fig. 6, which reveals, for example, that when the preferred mixing height range is exceeded in July, it is almost always because heights are too high, rather than too low (consistent with solar radiation being seasonally strong during the day in summer). Thus, above-range mixing heights are the most common cause of non-preferable conditions in July (c.f. Fig. 4), whereas below-range transport winds provide a secondary cause then.

Moving to October, the situation changes character in that transport wind conditions account for more of the non-preferable times than in July. The distribution of non-preferred wind

conditions, in this case, depends on location, with higher (lower) than preferred winds being the most common type in the north-west (south-east) portion of the study region. Enhancement of high wind conditions is also seen along the eastern flanks of the central Appalachian Mountains in October.

High winds continue to characterise the eastern Appalachian flanks in January, at which time the transport wind distribution has character (pattern) similar to that seen in October, just with fewer low wind conditions in most locations. An exception to this pattern is the North Carolina Piedmont region, which continues to experience more low than high out-of-range wind conditions in January (as is the case in October). The January mixing height climatology differs from October in that the

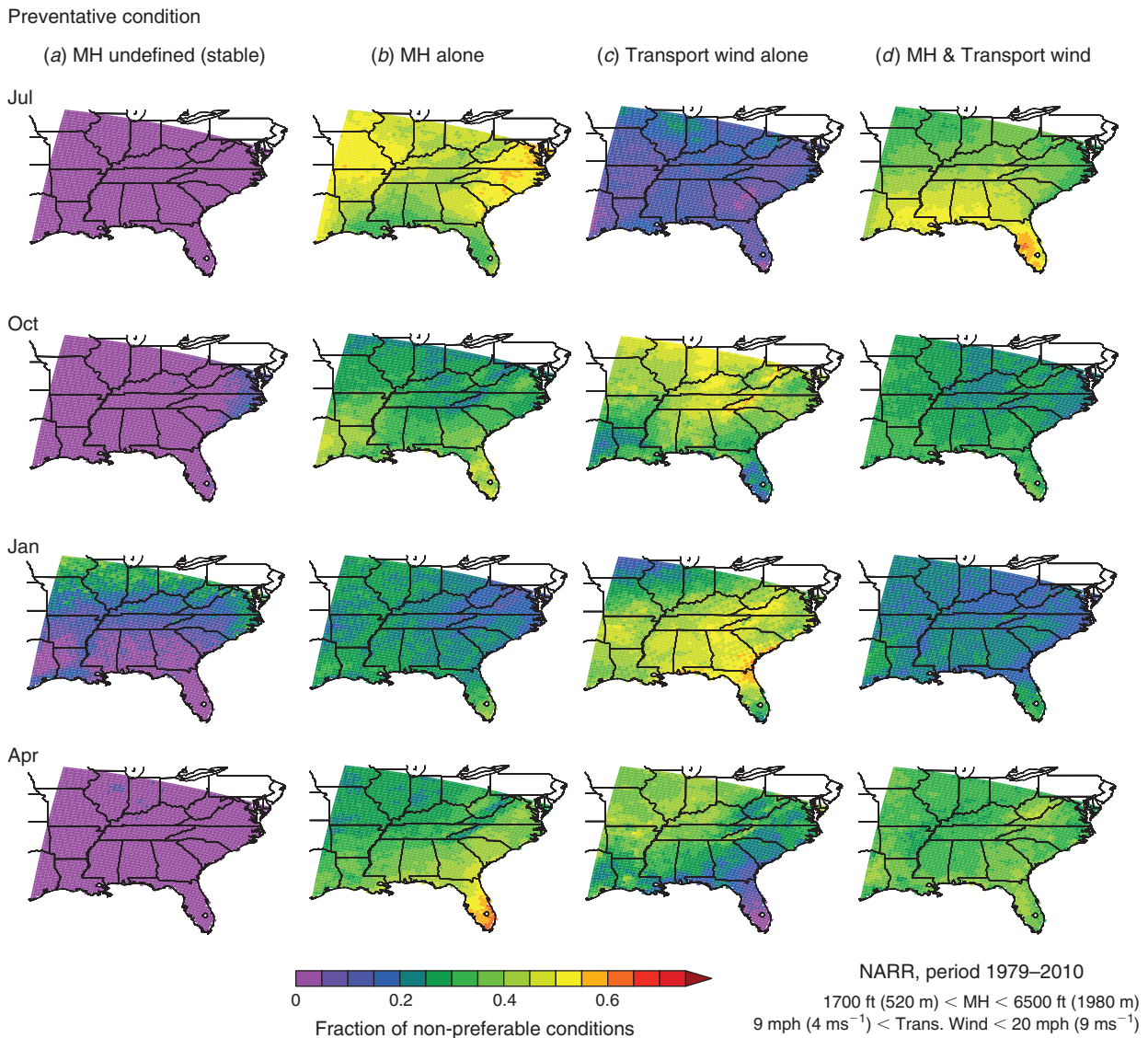


Fig. 4. Frequency of mixing height (MH) and transport wind conditions causing the preferred window to be exceeded. The four possibilities in this case include that, (column a) the mixing height is undefined because the atmospheric virtual potential temperature profile remains stable, (column b) the mixing height is defined, but is either too high or low, (column c) the transport wind is either too strong or weak, (column d) both mixing height and transport wind exceed the preferred range. Calculated based on North American Regional Reanalysis (NARR) data.

out-of-range heights, although a secondary cause of non-preferred conditions in both months, switch from being generally too high in October to being too low over most of the region in January. The notable exception in this case is that the Florida Peninsula, which evidently still receives enough sun in winter to sustain appreciable surface- to mid-tropospheric convection activity, continues to be characterised by relatively high mixing heights.

In April, a mix of higher than preferred mixing heights and stronger than preferred transport winds generally account for most of the non-preferred times. Low winds only account for more than half of the out-of-range cases over Florida and along the southern edges of Alabama and Georgia. Appalachian Mountain wind effects also are evident in April.

The comparable set of results based on CFSR data (Fig. 7) generally confirm those based on NARR in terms of the seasonality of the extremes. For example, by both datasets, out-of-range heights generally tend to be above threshold in July, October and April, but below threshold in January (except over the Florida Peninsula). Changes in character of the wind distribution across the Appalachian Mountains are also evident in the CFSR set of results, but are not quite as distinct as in the NARR case, which is offered at higher spatial resolution.

Near surface humidity, wind speed and daily precipitation effects

We also screened the set of times with preferable mixing height and transport winds for days in which prescribed burning would

Preventative condition

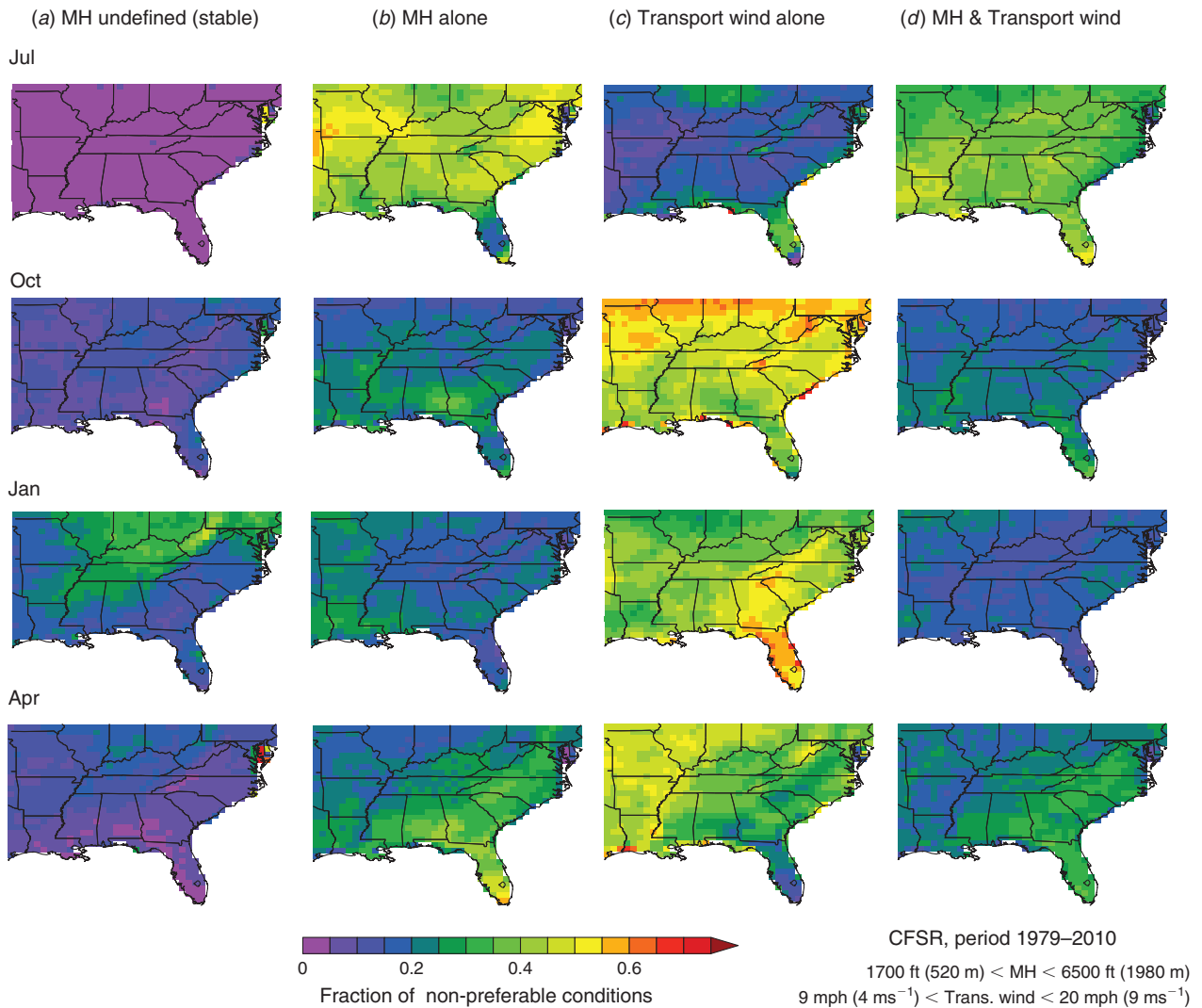


Fig. 5. Same as Fig. 4, except based on Climate Forecast System Reanalysis (CFSR) rather than North American Regional Reanalysis data.

likely be otherwise prevented due to high near surface wind [20 ft (6.1 m) wind speeds ≥ 20 mph (9 m s^{-1})] or low relative humidity ($\leq 20\%$) extremes. However, we found that such days are generally rare; specifically $< 0.5\%$ of days in a region averaged sense, would be removed from the prescribed burn window based on additional screening for these wind and humidity extremes. The lack of much effect due to the additional high near surface wind screen is consistent with the fact that we have already screened for transport winds > 20 mph (9 m s^{-1}) and surface wind speeds are typically less than those aloft.

Screening the same set of times for daily average precipitation > 6.35 mm (~ 0.25 inch), however, has a larger effect. In this case, the number of unique times affected (i.e. those with preferable mixing heights and transport winds, but > 6.35 mm of daily rain) varies considerably with season (Table 1). This rain effect has a wintertime minimum of only $\sim 1\%$ (2% based NARR (CFSR) data, but larger effects occur in June and July. In these months,

averaged over the study region, an additional 5–6% of possible times are removed from the preferred window.

The spatial distribution of times uniquely excluded from the prescribed burn window due to precipitation is shown for July in Fig. 8, along with the mean distribution of days with > 6.35 mm of rain. The concentration of rainy days, as well as their effect on the prescribed burn window exhibits two maxima: one along the south-east coast, and another in the interior, surrounding the central Appalachian Mountains.

The effects of precipitation activity in the interior are similar regardless of whether the NARR or CFSR data are used (Fig. 8), with localised values of up to an additional $\sim 10\%$ of times classified as non-preferable based on rain alone. Along the southern coast, however, the precipitation effects are much more evident in the CFSR than NARR case. This is because the NARR case contains a greater fraction of rainy days (compared with CFSR) that are already identified as non-preferable based on

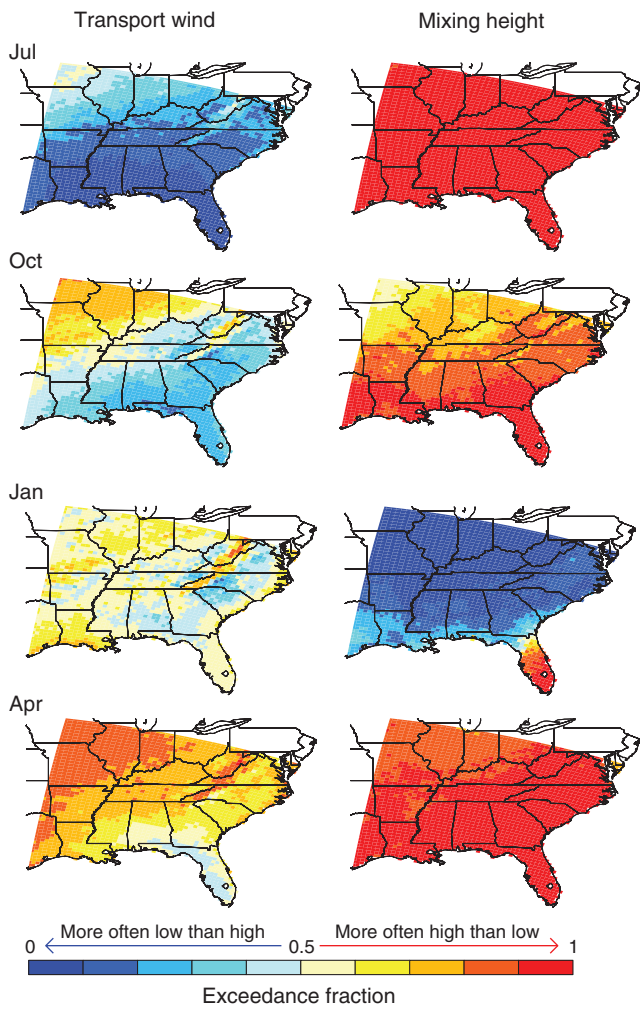


Fig. 6. Fraction of non-preferable conditions, by month, that exceed the preferred upper threshold (1 minus the value shown equals the fraction that fall below the lower threshold). Based on North American Regional Reanalysis data.

having above-threshold mixing heights. Effects of rain along the Gulf and Atlantic coasts are nonetheless still evident in the NARR result, just with lower amplitude and along a thinner stretch of the coastal plain, compared with the CFSR case.

Interannual variability

To gauge the extent to which the prescribed burn weather window varies interannually, we examined the standard deviation of the fraction of prescribed-burn-preferable times available over the 1979–2010 period, on a month-by-month basis. We found that the levels of interannual variability (not shown for brevity) are generally more homogenous over space and season (e.g. summer levels basically comparable to dormant season levels in this case) compared with the mean fields discussed above. Because of this, the ratio of the interannual variability to the monthly (or seasonal) mean, specifically:

$$\sigma_X / \langle X_i \rangle \tag{E1}$$

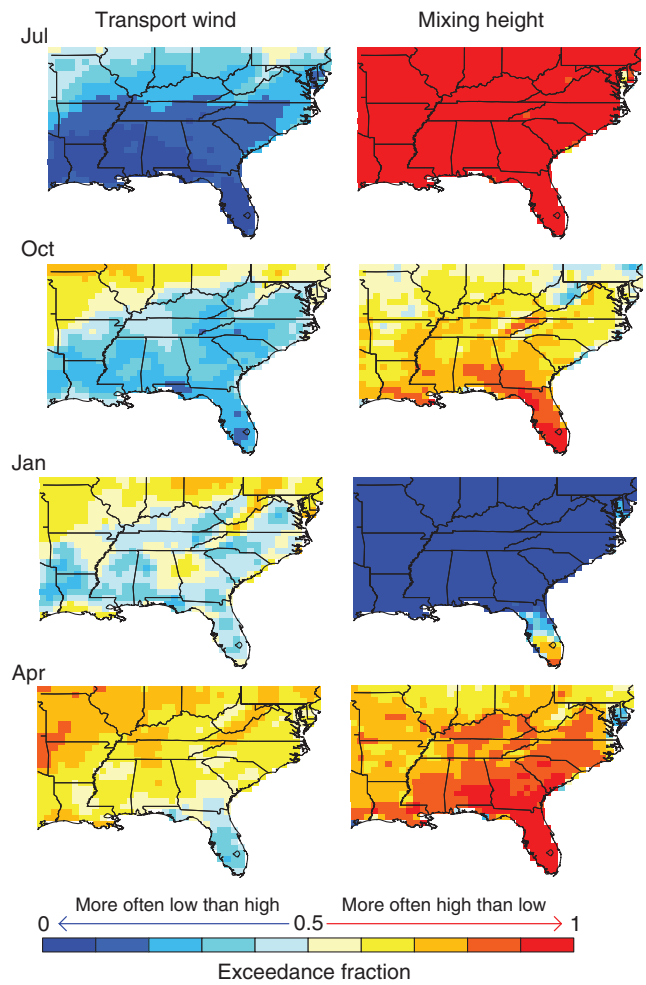


Fig. 7. Same as Fig. 6, except based on Climate Forecast System Reanalysis data.

Table 1. Precipitation effects on the prescribed burn window

Listed values give the regionally averaged percentage of times, per month, identified as unavailable for prescribed burning based on heavy (>6.35 mm day⁻¹) precipitation alone (period 1979–2010)

| Reanalysis | Jan | Feb | Mar | Apr | May | Jun | Jul | Aug | Sep | Oct | Nov | Dec |
|------------|-----|-----|-----|-----|-----|-----|-----|-----|-----|-----|-----|-----|
| NARR (%) | 1.1 | 1.9 | 3.5 | 4.1 | 4.8 | 5.2 | 5.2 | 4.3 | 4.1 | 3.3 | 2.4 | 1.1 |
| CFSR (%) | 1.9 | 2.6 | 3.3 | 3.6 | 4.9 | 6.0 | 5.6 | 4.4 | 4.2 | 3.2 | 2.7 | 1.8 |

where X is the fraction of times available over a given month i , the angled brackets represent taking the average over the 32 years considered, and σ is the standard deviation calculated based on the 32 monthly averages, varies across season largely as the inverse of the climatological monthly prescribed burn window. Thus, there is a peak in this normalised standard deviation in summer when the burn window (the denominator in Eqn 1) is smallest. Regionally averaged values of the normalised standard deviation are listed in Table 2 by month, and

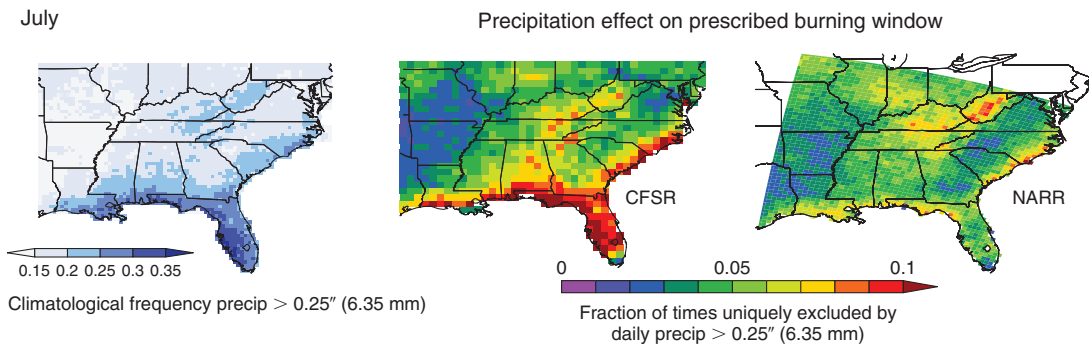


Fig. 8. Left: July climatological average frequency of daily rainfall >0.25 inch (6.35 mm). Middle: Fraction of times uniquely excluded from the prescribed burn window by >0.25 inch (6.35 mm) of rain based on the Climate Forecast System Reanalysis (CFSR). Right: unique times excluded based on the North American Regional Reanalysis (NARR).

Table 2. Interannual variability of the prescribed burn window

The interannual variability of the prescribed burn window estimated based on the standard deviation of times available, per month, for prescribed burning over the Southeast (period 1979–2010): values listed have been normalised (divided by) their respective climatological monthly means

| Jan | Feb | Mar | Apr | May | Jun | Jul | Aug | Sep | Oct | Nov | Dec |
|---|------|------|------|------|------|------|------|------|------|------|------|
| Climate Forecast System Reanalysis base case | | | | | | | | | | | |
| 0.34 | 0.30 | 0.27 | 0.32 | 0.42 | 0.51 | 0.58 | 0.59 | 0.39 | 0.27 | 0.27 | 0.31 |
| Climate Forecast System Reanalysis with precipitation | | | | | | | | | | | |
| 0.44 | 0.38 | 0.36 | 0.42 | 0.60 | 0.84 | 1.04 | 0.95 | 0.55 | 0.36 | 0.35 | 0.40 |
| North American Regional Reanalysis base case | | | | | | | | | | | |
| 0.25 | 0.23 | 0.25 | 0.33 | 0.46 | 0.52 | 0.55 | 0.56 | 0.45 | 0.29 | 0.20 | 0.24 |
| North American Regional Reanalysis with precipitation | | | | | | | | | | | |
| 0.37 | 0.31 | 0.34 | 0.45 | 0.66 | 0.92 | 0.98 | 0.95 | 0.64 | 0.37 | 0.29 | 0.32 |

include the raw mixing height and transport wind case, as well as the case with additional screening for extreme humidity, surface wind speed and rain. The salient result here is that, regardless of which dataset is used, the normalised standard deviation is near unity in the summertime, especially when precipitation effects are included. This effectively means that summer months from one year to the next can change in many locations from being almost entirely closed off to prescribed burn treatment in one year, to being about as open as mean winter conditions in another.

El Niño associations

Over the study period considered here, there are four ‘OLR El Niño events’ (1982–83, 1986–87, 1991–92 and 1997–98). Distinguishing these 4 years leaves several others that have El Niño status based on common El Niño definitions, but are not distinct based on OLR. We refer to this second subset of years as the ‘non-OLR’ El Niño years.

We performed a composite anomaly analysis of the fraction of times available for prescribed burns, based on averages over the traditional seasons (Jun–Jul–Aug, or ‘JJA’, Sep–Oct–Nov, or ‘SON’, etc.), and the four OLR-identified El Niño years, as well as the other non-OLR El Niño years. We define the non-OLR years in this case as those that currently have El Niño status based on 3-month running mean central tropical Pacific SST

anomaly >0.5°C (as listed at http://www.cpc.ncep.noaa.gov/products/analysis_monitoring/ensostuff/ensoyears.shtml, accessed 1 April 2017), but are not distinct based on OLR. We have performed the analysis on both the base case (mixing height and transport wind alone) and additionally screened set of results and found qualitatively very similar results in each case. For this reason, only one set (additionally screened) is discussed herein.

The non-OLR El Niño composites do not contain enough locally statistically significant anomalies to reach regional statistical significance at even very low confidence levels (e.g. 66%) in any of the four seasons considered. Evidently, there is not a very useful association between this type of tropical Pacific anomaly state and the variability of prescribed burn window that we calculate over the Southeast.

Composites based on the OLR El Niño years, in contrast, do exhibit enough locally statistically significant anomaly to reach regional statistical significance at the 80% level, or better, in three of four seasons based on the CFSR data (left half of Fig. 9). Specifically, JJA (Year 0), DJF (Year 0–1) and MAM (Year 1) reaches this level of regional statistical significance, but SON (Year 0; not shown) does not. The CFSR-based anomaly amplitudes that reach local statistical significance at the 90% confidence level, or higher, are shown in Fig. 9 (second column from left). Locally statistically significant anomaly is found over much of the south-eastern portion of the study area in each

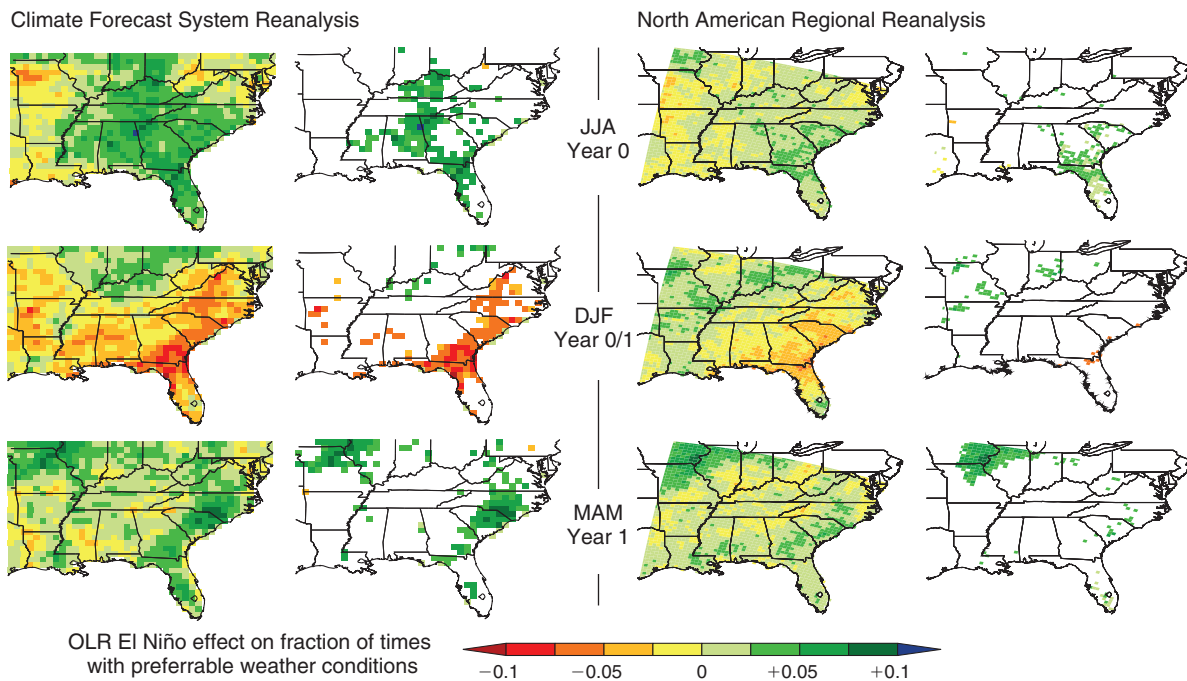


Fig. 9. Outgoing longwave radiation (OLR) El Niño composite seasonal anomalies for Jun–Aug (JJA), Dec–Feb (DJF), and Mar–May (MAM). Anomalies are masked at the 90% confidence interval based on amplitude in the second and fourth columns from the left, with full fields shown in the 1st and 3rd columns. Green (red) shading indicates higher (lower) than usual number of times with prescribed-burn-preferable weather during El Niño years, compared with the all-year average for the given season.

of these three seasons. There is, interestingly however, a change of sign between summer and winter, and then again between winter and spring, such that an anomalously narrow prescribed burn window is associated with the OLR El Niño years in winter (DJF), but wider windows seen the preceding summer (JJA Year 0) and following spring (MAM Year 1). The reason for this change in sign can be understood based on the information presented in Fig. 7, and the fact that inspection of each affected season showed that the associated mixing height composite was anomalously low over the strongly affected region. Because there is a switch in tendency for mixing heights to be too high in summer and spring, but too low in winter (except over southern Florida; Fig. 7) the reduction in number of high-mixing-height times that is associated with the OLR El Niño events has the net effect of making more days available for prescribed burns in spring and summer, but fewer days available in winter.

The comparable set of results based on NARR data (right half of Fig. 9) agree quite well with the CFSR results in terms of their anomaly pattern, but differ in terms of the total number of days affected. Specifically, the NARR-based composite anomalies have amplitudes that are generally smaller than in the CFSR case, and contain much less locally statistically significant anomaly. This suggests that we can have confidence in the character of the OLR El Niño association over this time, but more work is needed to determine its amplitude relative to other sources of variability.

Discussion

This work has quantified, with focus on mixing height and transport wind conditions calculated from a pair of numerical

weather model reanalyses, the mean seasonal variation of weather conditions preferable for prescribed burn treatment of wildlands across the Southeastern USA. Results reveal a 5-fold or larger change in the occurrence frequency of such conditions over the course of the mean seasonal cycle over much of the core Southeast. Minima in availability occur over most of the region in summer and maxima occur in autumn or winter. Localised departure from the regional-mean seasonal cycle is evident in some areas, including the Florida Peninsula and along flanks of the Appalachian Mountains.

The summertime minimum is attributable mainly to the tendency for mixing heights to reach above-threshold levels then. Upper limits on mixing height are in place to limit erratic fire behaviour. In winter, however, the main reason preventing prescribed burning, based on our results, is that transport winds fall out of range. Above (erratic fire behaviour risk) and below (insufficient smoke dispersion) threshold transport wind conditions, in roughly similar numbers, act to disrupt the prescribed burn window in winter, with the exception of some localised enhancements near the Appalachian Mountains.

We also screened our base-case distribution of prescribed burn preferable times for additional days in which applied fire treatment might be otherwise prevented due to heavy precipitation on the intended day of ignition. Because sufficiently rainy days mainly occur in summer, this rain effect further narrows the already slim summertime weather window, thereby adding to the seasonal variation already set by the mixing height and transport wind conditions.

The criteria for the preferred prescribed burn weather conditions used here are based on now-longstanding rules (Wade

and Lunsford 1989) meant to limit adverse effects on breathable air quality and erratic fire behaviour, along with the difficulty inherent in attempting effective application of fire during heavy rain. Thus, we used criteria chosen to be relevant to a wide variety of terrain, fuel types and objectives. Accordingly, our calculations may not be fully comprehensive. Particularly, adverse fuel moisture conditions, such as those associated with a major drought, would further limit the opportunity for prescribed burning beyond the window of opportunity identified by our calculations. Additionally, dependent on fuel type and location, additional time (days), following heavy rain may be needed in order that fuel moisture contents reach levels conducive to the given treatment objectives. We calculated the effect of (possibly) screening for additional drying time following rainy days (we used a suggested rule of 1 day per 5.08 mm (~0.2 inches) of precipitation). Results in this case highlighted prescribed burns taking place in the fall and winter along the Gulf coastal plain, due to the relative openness of the window then, and the fact that some of the heavier rains occur in the Gulf coast region during the cool season. Pers. comm. with colleagues with extensive practical experience conducting burns in this region, along with the coauthor's (J. M. Varner) own experience, strongly suggests that an additional post-rain screen like this, if applied generally across this region, would produce misleading results. More work is needed to understand the predictability of fuel moisture effects on our ability to conduct effective and controlled prescribed burns across the Southeast.

The seasonal march of the prescribed burn weather window described here has implications to management objectives, especially those that require treatment to occur in a specific season to be most effective. There is wide discussion over the timing or season of burning across the Southeast (Hiers *et al.* 2000; Knapp *et al.* 2009; Ryan *et al.* 2013; Kobziar *et al.* 2015; Platt *et al.* 2015). A major shift throughout the region has been to attempt to burn more during the growing season (late spring and summer) to mimic prehistoric ignition timing (as reconstructed from fire scar evidence; see Stambaugh *et al.* 2011 but see Stambaugh *et al.* 2017 for a greater regional discussion of fire timing). Our results highlight some barriers to doing this that are presented by the seasonality of the preferred weather window. Over much of the Southeast, the season often preferred for burning from a forest health and function perspective is also the season in which it is hardest to find the specific weather conditions that enable effective and controlled application of fire. Our analysis highlights the difficulty that managers face when season-of-burn narrows the potential burn days in an already slim period.

We anticipate that these results will motivate some discussion of the risks and benefits associated with relaxing the preferred fire weather criteria in order to lessen this difficulty. Knowledge of the sensitivity of the burn day climatology to the possible changes will be needed for an informed discussion to occur. Preliminary results, based on recalculating our prescribed burn window climatology after changing mixing height limits, suggest that the constraint mainly responsible for narrowing the growing season window (upper limit mixing height) may be one of the most efficient in terms of its percentage of days-gained per limit-increase. We are at work analysing the many cases (i.e. calculating rates of change for the upper and lower limits of

mixing height and transport wind across 12 months) necessary to complete this companion study.

The availability of preferable times for prescribed burning varies substantially on interannual timescales. In summer, the interannual standard deviation is nearly as large as the climatological monthly average, meaning that the prescribed burn window can be effectively closed in summer in some years, but much more open in others. Especially if foreseeable, this variation could be capitalised on when these favourable conditions occur, reducing pressures for growing season burning during years when prescribed burning windows are exceedingly narrow. Our results offer some potential pathways for doing this.

We have evaluated this interannual variability for its possible linkage to El Niño events in the tropical Pacific and found that the same subset of El Niño event years that has been shown previously to account for most of the useful linkage to US seasonal temperature and precipitation anomaly over the study period (i.e. the 'OLR El Niño events' of 1982–83, 1986–87, 1991–92, 1997–98) have an at least moderately statistically strong (reach 80% confidence in a regionally averaged sense) connection to the year-to-year prescribed burn window variability over the Southeast, based on the CFSR data. The NARR-based composite interannual anomaly results agree with the CFSR results in character (pattern), but contain less locally statistically significant anomaly, suggesting that more work is needed to gauge the actual amplitude strength of this connection.

The other 'non-OLR' El Niño years produce composites that do not reach regional statistical significance at even a much more lenient 66% confidence interval, regardless of which dataset is used. This suggests that other sources of variability than those emanating from the tropical Pacific control the anomalies seen over the Southeastern USA in these other years.

The CFSR and NARR set of results agree that the OLR El Niño association is characterised by lower than average mixing heights over the affected seasons and regions. Because of changes in the relationship between the seasonal-mean mixing height and the (constant) preferred mixing height range, this lower-than-average mixing height association causes alternate widening and narrowing of the prescribed burn weather window depending on season. Specifically, preferable weather conditions are less frequent in winter (Year 0–1), but more frequent in the preceding summer (Year 0) and following spring (Year 1).

Previous studies (e.g. Brenner 1991; Dixon *et al.* 2008) have found associations between El Niño events and decreases in fire activity in the Southeast, especially near the beginning of the calendar year (Goodrick and Hanley 2009). El Niño effects on precipitation have often been hypothesised to explain these associations. Our results suggest that, in addition to precipitation effects, the identified mixing height associations (particularly decreases around the end of the calendar year) may play a role. It is important to note, however, that not all commonly considered El Niño years are associated with the identified regional weather associations; it is the OLR-identified subset of events that account for them.

The aforementioned OLR El Niño index has typically distinguished the OLR event years from others in time to be of use to winter, and later seasonal forecasting efforts, without the need to forecast OLR. To the extent the behaviour seen in this study period holds in future decades, the OLR El Niño winter

and spring associations described here offer a direct statistical basis for issuing winter (Year 0–1) and spring (Year 1) fire weather forecasts. Our results are based on the recent multi-decadal period over which OLR has been available from satellites. The equatorial Pacific has been observed to exhibit large multidecadal variability (Harrison and Chiodi 2015) and been hypothesised to be undergoing longer term change (Cai *et al.* 2015). Thus, it will be necessary to monitor the relationships described here to determine the extent to which they continue to offer a useful basis for seasonal forecasting in future decades. To be useful in summer, even in the event that the relationships hold, this approach would require learning to predict OLR anomaly development over the tropical Pacific.

Conclusions

The climatological variation of the prescribed burn weather window (“burn days”) over the Southeastern USA exhibits large spatial gradients associated with distinct geographical features (e.g. Appalachian Mountains, Florida Peninsula) as well as strong seasonality. In a region-averaged sense, burn days are most frequent in the dormant (winter) season and much less common (by factor of ~3) in the summer. There is also strong interannual variability, such that summer months can alternate from having, in many locations, nearly zero burn days in one year, to having as many burn days as mean winter conditions in another. Composite analysis identified a tendency for lower than average mixing heights to occur during OLR El Niño events. Over the affected region, this El Niño association has the effect of increasing burn day availability in summer of Year 0 and spring of Year 1, but reducing it in winter Year 0–1.

These results, which identify spatial and temporal patterns in the burn day climatology – as well as the influence of the El Niño–Southern Oscillation on interannual variability, offer some promise for prescribed fire planning in the region. Despite the extensive prescribed burning that takes place in the Southeast, managers report that they fail to meet their goals for frequency (Kobziar *et al.* 2015). This same methodology could be employed in other fire-prone regions where management objectives fail to be met due to narrow prescribed burn windows (Quinn-Davidson and Varner 2012; Ryan *et al.* 2013). Focusing resources and personnel to match annual patterns in burn days and capitalising on years with greater than average availability would enable more prescribed burning to meet landscape restoration and management goals.

Conflicts of interest

The authors declare that they have no conflicts of interest.

Acknowledgements

This work was supported through funding from the USA National Fire Plan, with additional support for A. M. Chiodi by the Joint Institute for the Study of the Atmosphere and Ocean under NOAA Cooperative Agreements NA17RJ1232 and NA10OAR4320148, and the Ocean Observing and Monitoring Division of the NOAA Climate Program Office (FundRef number 100007298). Discussions with P. G. Dixon helped stimulate this work. B. E. Potter provided thoughtful comments on an earlier draft. The presentation of results was improved by the thoughtful comments of three anonymous reviewers.

References

- Brenner J (1991) Southern Oscillation anomalies and their relationship to wildfire activity in Florida. *International Journal of Wildland Fire* **1**, 73–78. doi:10.1071/WF9910073
- Brown TJ, Hall BL (2010) Verification of North Carolina mixing height forecasts for smoke management, final report. Program for Climate, Ecosystem and Fire Applications, Desert Research Institute. (Reno, NV, USA)
- Cai W, Santoso A, Wang G, Yeh S-W, An S-I, Cobb KM, Collins M, Guilyardi E, Jin F-F, Kug J-S, Lengaigne M, McPhaden MJ, Takahashi K, Timmerman A, Vecchi GA, Watanabe M, Wu L (2015) ENSO and greenhouse warming. *Nature Climate Change* **5**, 849–859. doi:10.1038/NCLIMATE2743
- Chiodi AM, Harrison DE (2010) Characterizing warm-ENSO variability in the equatorial Pacific: an OLR perspective. *Journal of Climate* **23**, 2428–2439. doi:10.1175/2009JCLI3030.1
- Chiodi AM, Harrison DE (2013) El Niño impacts on seasonal US atmospheric circulation, temperature and precipitation anomalies: the OLR-event perspective. *Journal of Climate* **26**, 822–837. doi:10.1175/JCLI-D-12-00097.1
- Chiodi AM, Harrison DE (2015) Global seasonal precipitation anomalies robustly associated with El Niño and La Niña events – an OLR perspective. *Journal of Climate* **28**, 6133–6159. doi:10.1175/JCLI-D-14-00387.1
- Chiodi AM, Bond NA, Larkin NK, Barbour RJ (2016) Summertime rainfall events in eastern Oregon and Washington. *Weather and Forecasting* **31**, 1465–1480. doi:10.1175/WAF-D-16-0024.1
- Dixon PG, Goodrich GB, Cooke WH (2008) Using teleconnections to predict wildfires in Mississippi. *Monthly Weather Review* **136**, 2804–2811. doi:10.1175/2007MWR2297.1
- Fearon MG, Brown TJ, Curcio GM (2015) Establishing a national standard method for operational mixing height determination. *Journal of Operational Meteorology* **3**, 172–189. doi:10.1519/NWAJOM.2015.0315
- Goodrick SL, Hanley D (2009) Revisiting the relationship between Florida wildfire activity and ENSO. *International Journal of Wildland Fire* **18**, 476–482. doi:10.1071/WF07034
- Goodrick SL, Achtemeier GL, Larkin NK, Liu Y, Strand TM (2013) Modelling smoke transport from wildland fires: a review. *International Journal of Wildland Fire* **22**, 83–94. doi:10.1071/WF11116
- Haines TK, Busby RL, Cleaves DA (2001) Prescribed burning in the South: trends, purpose and barriers. *Southern Journal of Applied Forestry* **25**, 149–153.
- Hardy CC, Ottmar RD, Peterson JL, Core JE, Seamon P (2001) Smoke management guide for prescribed and wildland fire: 2001 edition. National Wildfire Coordination Group, PMS 420–2. (Boise, ID, USA)
- Harrison DE, Chiodi AC (2015) Multi-decadal variability and trends in the El Niño–Southern Oscillation and tropical Pacific fisheries implications. *Deep-sea Research – II. Topical Studies in Oceanography* **113**, 9–21. doi:10.1016/J.DSR2.2013.12.020
- Harrison DE, Chiodi AC (2017) Comment on ‘Characterizing ENSO coupled variability and its impact on North American seasonal precipitation and temperature’ by L’Heureux, Tippet, and Barnston *Journal of Climate* **30**, 427–436. doi:10.1175/JCLI-D-15-0678.1
- Hiers JK, Wyatt R, Mitchell RJ (2000) The effects of fire regime on legume reproduction in longleaf pine savannas: is a season selective? *Oecologia* **125**, 521–530. doi:10.1007/S004420000469
- Higgins RW, Shi W, Yarosh E, Joyce R (2000) Improved United States precipitation quality control system and analysis. NCEP/Climate Prediction Center Atlas **7**. Available at http://www.cpc.ncep.noaa.gov/research_papers/ncep_cpc_atlas/7/toc.html [Verified 1 January 2017]
- Holzworth GC (1964) Estimates of mean maximum mixing depths in the contiguous United States. *Monthly Weather Review* **92**, 235–242. doi:10.1175/1520-0493(1964)092<0235:EOMMMD>2.3.CO;2

- Holzworth GC (1967) Mixing depths, wind speeds and air pollution potential for selected locations in the United States. *Journal of Applied Meteorology* **6**, 1039–1044. doi:10.1175/1520-0450(1967)006<1039:MDWSAA>2.0.CO;2
- Knapp EE, Estes BL, Skinner CN (2009) Ecological effects of prescribed fire season: a literature review and synthesis for managers. USDA Forest Service, Albany, CA. General Technical Report PSW-GTR-224.
- Kobziar LN, Goodwin D, Taylor L, Watts AC (2015) Perspectives on trends, effectiveness, and impediments to prescribed burning in the Southern US. *Forests* **6**, 561–580. doi:10.3390/F6030561
- Larkin NK, Harrison DE (2002) ENSO warm (El Niño) and cold (La Niña) event life cycles: ocean surface anomaly patterns, their symmetries, asymmetries, and implications. *Journal of Climate* **15**, 1118–1140. doi:10.1175/1520-0442(2002)015<1118:EWENOA>2.0.CO;2
- Lavdas LG (1986) An atmospheric dispersion index for prescribed burning. USDA Forest Service, Southeastern Forest Experiment Station, Research Paper SE-256. (Macon, GA, USA)
- Melvin MA (2015) National prescribed fire use survey report. (Coalition of Prescribed Fire Councils, Inc.)
- Mesinger F, DiMego G, Kalnay E, Mitchell K, Shafran PC, Ebisuzaki W, Jović D, Woollen J, Rogers E, Berbery EH, Ek MB, Fan Y, Grumbine R, Higgins W, Li H, Lin Y, Manikin G, Parrish D, Shi W (2006) North American regional reanalysis. *Bulletin of the American Meteorological Society* **87**, 343–360. doi:10.1175/BAMS-87-3-343
- Platt WJ, Orzell SL, Slocum MG (2015) Seasonality of fire weather strongly influences fire regimes in south Florida savanna-grassland landscapes. *PLoS One* **10**, e0116952. doi:10.1371/JOURNAL.PONE.0116952
- Quinn-Davidson LN, Varner JM (2012) Impediments to prescribed fire across agency, landscape and manager: an example from northern California. *International Journal of Wildland Fire* **21**, 210–218. doi:10.1071/WF11017
- Rasmusson EM, Carpenter TH (1982) Variations in tropical sea surface temperature and surface wind fields associated with the Southern Oscillation/El Niño. *Monthly Weather Review* **110**, 354–384.
- Ropelewski CF, Halpert MS (1996) Quantifying Southern Oscillation–precipitation relationships. *Journal of Climate* **9**, 1043–1059. doi:10.1175/1520-0442(1996)009<1043:QSOPR>2.0.CO;2
- Ryan KC, Knapp EE, Varner JM (2013) Prescribed fire in North American forests and woodlands: history, current practice, and challenges. *Frontiers in Ecology and the Environment* **11**, e15–e24. doi:10.1890/120329
- Saha S, Moorthi S, Pan H-L, Wu X, Wang J, Nadiga S, Tripp P, Kistler R, Woollen J, Behringer D, Liu H, Stokes D, Grumbine R, Gayno G, Wang J, Hou Y-T, Chuang H-Y, Juang H-MH, Sela J, Iredell M, Treadon R, Kleist D, Van Delst P, Keyser D, Derber J, Ek M, Meng J, Wei H, Yang R, Lord S, van den Dool H, Kumar A, Wang W, Long C, Chelliah M, Xue Y, Huang B, Schemm J-K, Ebisuaki W, Lin R, Xie P, Chen M, Zhou S, Higgins W, Zou C-Z, Liu Q, Chen Y, Han Y, Cucurull L, Reynolds RW, Rutledge G, Goldberg M (2010) The NCEP climate forecast system reanalysis. *Bulletin of the American Meteorological Society* **91**, 1015–1058. doi:10.1175/2010BAMS3001.1
- Seibert P, Beyrich F, Gryning S-E, Joffre S, Rasmussen A, Tercier P (2000) Review and intercomparison of operational methods for the determination of the mixing height. *Atmospheric Environment* **34**, 1001–1027. doi:10.1016/S1352-2310(99)00349-0
- Stambaugh MC, Guyette RP, Marschall JM (2011) Longleaf pine (*Pinus palustris* Mill.) fire scars reveal new details of a frequent fire regime. *Journal of Vegetation Science* **22**, 1094–1104. doi:10.1111/J.1654-1103.2011.01322.X
- Stambaugh MC, Varner JM, Jackson ST (2017) Biogeography: an interweave of climate, fire, and humans. In ‘Ecological restoration and management of longleaf pine forests’. (Eds L.K. Kirkman and S.B. Jack) pp.17–38. (CRC Press/Taylor & Francis: Boca Raton, FL, USA)
- Stull RB (1988) ‘An introduction to boundary layer meteorology.’ (Kluwer Academic Publishers: Boston, MA, USA)
- Stull RB (1991) Static stability – an update. *Bulletin of the American Meteorological Society* **72**, 1521–1529. doi:10.1175/1520-0477(1991)072<1521:SSU>2.0.CO;2
- Turner JA, Lawson BD (1978) Weather in the Canadian forest fire danger rating system. A user guide to national standards and practices. B.D. Fisheries and Environment Canada, Canadian Forest Service, Pacific Forest Research Centre, Information Report BC-X-177. (Victoria, BC, Canada)
- Wade DD, Lunsford JD (1989) A guide for prescribed fire in southern forests. USDA Forest Service, Southern Region, Technical Publication R8-TP 11.
- Waldrop TA, Goodrick SL (2012) Introduction to prescribed fires in the Southern ecosystems. USDA Forest Service, Southern Research Station, Science Update SRS-054. (Asheville, NC, USA)